

## **Modeling of Lunar Dust Contamination Due to Plume Impingement**

Michael Woronowicz

SGT Inc., 7701 Greenbelt Road, Greenbelt, Maryland 20770, USA  
michael.s.woronowicz@nasa.gov

Historical data from the Apollo missions indicate the ubiquitous presence of lunar dust caused a number of troubling performance issues, including degradation of mechanisms, optical elements, and thermal control devices. Consequently, NASA Constellation program managers are interested in developing designs, techniques, and procedures to mitigate the deleterious effects of this material when humans return to the Moon.

One particular scenario involves the first Altair Lunar Lander descent operations, where the vehicle's engine plume will disturb electrically charged lunar regolith particulates, some of which may subsequently become attracted to the lander itself. Of special concern is that enough particles may find their way to thermal control surfaces, degrading their function to unacceptable levels.

It is planned to develop a model for this particular case and use it to study the influence of such effects as engine height above the Moon's surface, effect of thrust level, and thrust vector angle during descent and ascent operations. Lunar dust size distribution and other properties will be considered to determine the fraction of particles of a given size transported to critical Altair surfaces. Electrical charging and field effects must also be considered.

A transient plume model must be used for this study, and an initial approach for this facet is discussed. The effect of electric fields on charged particle trajectories will follow a technique developed for satellite contamination in the NASA Space Environments & Effects program.

## 1.0 Introduction

The NASA Apollo program encountered a number of issues regarding human presence on the Moon due to the effects of lunar dust. The possibility of surface obscuration during critical landing sequences had been foreseen<sup>1,2</sup>, but during the Apollo missions it became apparent that lunar dust was a significant hazard. Among other things, dust-related problems included abrasion damage to gauge faces and helmet visors, mechanism clogging, development of space suit pressurization leaks, loss of radiator heat rejection capabilities to the point where vulnerable equipment exceeded maximum survival temperature ratings, and even temporary vision and respiratory problems for astronauts within the Apollo Lunar Module (LM)<sup>3-5</sup>.

In the absence of oxygen in the lunar atmosphere, dust particles often remain jagged once formed, and embed themselves in equipment quite readily. They also feature low electrical conductivity, so under high vacuum conditions they can retain a charge<sup>6</sup>. Therefore lunar dust adhesion properties are characterized by electrostatic as well as mechanical mechanisms, resulting in a tenacious ability to cling to a wide variety of materials<sup>6</sup>.

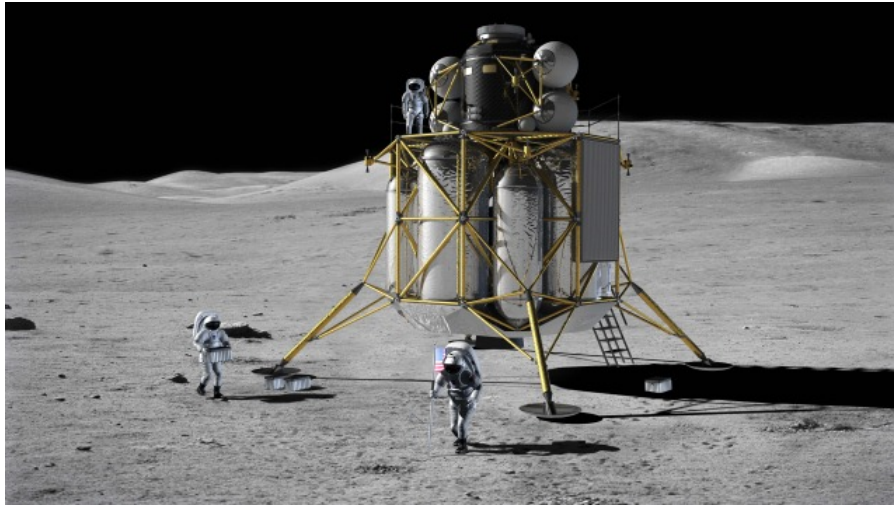


**Figure 1. NASA Altair Lunar Lander Concept (Ref. 7)**

The current NASA Constellation Program features many system-level components, including the Altair Lunar Lander (Fig. 1)<sup>7</sup>. Whereas the Apollo LM only endured conditions on the lunar surface for up to about three days, Altair is being designed to remain in this environment as long as seven days to support four astronauts in sortie operations, and 219 days in support of planned lunar outpost activities<sup>8</sup>. In particular, program managers are interested in plume-generated dust transport onto thermal control surface radiators of the first Altair created by its own landing operations.

The purpose of this paper is to describe current development efforts for modeling a self-contamination mechanism dealing with the non-line-of-sight (non-LOS) transport of charged lunar regolith particulate matter to deposit on surfaces such as the horizontal radiator located on the right side of the vehicle depicted in Fig. 1.

## 2.0 Model Formulation

The problem stated above consists of three parts. First the Altair descent engine's plume must be modeled as it interacts with the lunar surface. Second, plume impingement surface stresses need to be translated into a lunar

regolith particulate generation rate. Finally, the manner in which these particles find their way to Altair must be considered.

## 2.1 Lunar Plume Impingement

### 2.1.1 Descent Engine Model Parameters

As the Altair design is still under development, it is difficult to ascertain the precise descent engine that will be used. Recent reports indicate it will be a throttlable derivative of the versatile RL-10 liquid oxygen/liquid hydrogen (LOX/LH<sub>2</sub>) engine<sup>9,10</sup>. Because so many versions of the RL-10 have been developed and tested over the past 50 years, the author suspects yet another version may be created specifically for the Altair program. For the current modeling application, a set of parameters consistent with the RL-10A-4 engine were used (Table 1)<sup>11</sup>.

**Table 1. RL-10A-4 Engine Parameters (Ref. 11)**

<i>Item</i>	<i>Value</i>
Thrust [N]	92,500
Oxidizer/Fuel Mass Ratio (O/F)	5.5
Specific Impulse ( $I_{sp}$ ) [s]	449
Area Ratio	84
Chamber Pressure [Pa]	$3.9 \times 10^6$

In comparison to Table 1 parameters<sup>12</sup>, the descent engine on the Apollo LM utilized hypergolic propellants and achieved 44,000 N worth of thrust at  $I_{sp} = 311$  s. For vacuum-rated  $I_{sp}$  values, nozzle exit velocities are proportional to specific impulse. Thus it becomes clear that the bulk exit velocity of the Altair descent engine may be something like 44 percent higher than Apollo's LM, making it considerably more energetic even at equal propellant feed rates.

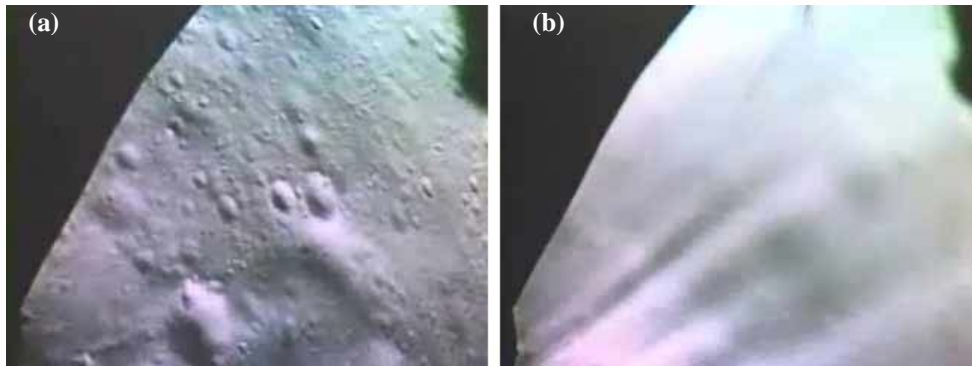


**Figure 2. Frames from Apollo 17 landing operation film; (a) relatively high altitude, and (b) final phase**

Recent photogrammetric analysis of Apollo descent operations filmed from within the LM show that lunar dust was ejected at angles of only 1-3 degrees off the surface<sup>13</sup> (Fig. 2). This blowing effect can only be stronger with the RL-10 engine. It is reasoned that the drag force on disturbed lunar dust particles must overwhelm any electrostatic attraction to the Altair vehicle, so one may neglect effects of the latter mechanism while the engine is operating. This assertion is apparently verified by observations from Ref. 13 for the LM descent engine. However, it is possible for lunar dust to reach Altair surfaces at the end of descent operations as the engine powers down. Regolith may still be disturbed during this transient, but at much lower degrees of entrainment. Charged particles that happen to be close enough may then become successfully attracted to the Lunar Lander.

### 2.1.2 Initial Plume Model

Unfortunately, analysis and simulation of gases expanding from rocket engines into high vacuum, or the effects plumes from these sources create when they interact with solid surfaces, present a sustained challenge to the scientific and engineering communities. As a plume expands into high vacuum, density levels, and hence collision rates, decrease rapidly by many orders of magnitude. Often, the difficulty lies in accurately describing a flowfield that passes from continuum flow at the nozzle exit, through the transition regime, to free molecule behavior within a relatively short distance downstream. In the current application, one must add transient effects to this mix.

Although powerful numerical techniques using direct simulation Monte Carlo (DSMC) and computational fluid dynamics (CFD) can provide detailed snapshots of steady behavior for the RL-10 engine plume and its interaction with the lunar surface, these results are obtained with great difficulty due to the large variations in plume properties and their gradients associated with the expansion, coupled with incident shock wave resolution and stresses associated with lunar surface interaction<sup>14</sup>. Nevertheless, it will be salutary to gain insights from results provided by such efforts.

In order to scope out the overall problem, initial efforts will make use of an analytic technique based on a set of point source, free molecule (FM) equations developed by Woronowicz to approximate flow exhausting from rocket nozzles<sup>15,16</sup>.

$$\frac{\partial f}{\partial t} + \mathbf{v} \cdot \frac{\partial f}{\partial \mathbf{x}} = Q_1; \quad Q_1 = \frac{2\beta^4}{A_1 \pi} \delta(\mathbf{x}) \dot{m}(t) |\mathbf{v} \cdot \hat{\mathbf{n}}| \exp(-\beta^2(\mathbf{v} - \mathbf{u}_e)^2); \quad (1)$$

$$A_1 \equiv e^{-s^2 \cos^2 \phi_e} + \sqrt{\pi} s \cos \phi_e (1 + \operatorname{erf}(s \cos \phi_e)).$$

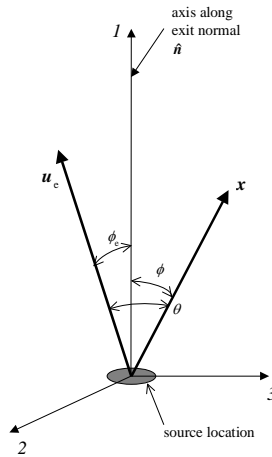


**Figure 3. Schematic representation of various quantities and angles used in analytical model**

$Q_1$  represents directed flow from a Lambertian, thermal velocity distribution superimposed on convective exit velocity  $\mathbf{u}_e$  for mass flow rate  $\dot{m}$ ,  $\beta \equiv 1/\sqrt{2RT}$ , and speed ratio  $s \equiv \beta u_e$ . Normal  $\hat{\mathbf{n}}$  represents the orientation of a local starting surface element, and  $\mathbf{v} \cdot \hat{\mathbf{n}}$  emphasizes the imposed directional constraint. Generally  $\mathbf{u}_e$  is not aligned with  $\hat{\mathbf{n}}$ , with the angle between the two defined by  $\phi_e$  (Fig. 3). Local angle  $\phi$  is measured between variable position  $\mathbf{x}$  (distance  $r$ , experiencing local velocity  $\mathbf{v}$ ) and  $\hat{\mathbf{n}}$ , and angle  $\theta$  is measured between  $\mathbf{u}_e$  and  $\mathbf{x}$ .

When  $\dot{m}$  in Eq. 1 is described by a Dirac Delta function  $\Delta m \delta(t)$ , one may solve for successive moments of molecular distribution function  $f$ , finding expressions for density  $\rho$ , mass flux  $\dot{\Phi}$ , incident normal momentum flux  $p_{\perp}$ , shear stress  $\tau$ . For an impinging surface element at location  $\mathbf{x}$ , incident fluxes make angle  $\psi$  with the local receiver normal.

$$\rho(\mathbf{x}, t) = \frac{2 \Delta m \beta^4}{A_1 \pi} \frac{r \cos \phi}{t^4} e^{w^2 - s^2} e^{-z^2}, \quad (2)$$

$$\dot{\Phi}(\mathbf{x}, t) = \frac{\rho r}{t} \cos \psi, \quad (3)$$

$$p_{\perp}(\mathbf{x}, t) = \frac{\rho r^2}{t^2} \cos \psi, \quad (4)$$

$$\tau(\mathbf{x}, t) = \frac{\rho r^2}{t^2} \sin \psi. \quad (5)$$

In Eq. 2,  $z \equiv \alpha - w$ ,  $\alpha \equiv \beta r/t$ , and  $w \equiv s \cos \theta$ . Eqns. 2-4 may be combined to obtain a free expansion expression for velocity  $v$  ( $\psi = 0$ ).

$$v(\mathbf{x}, t) = \frac{\dot{\Phi}(\mathbf{x}, t)}{\rho(\mathbf{x}, t)}. \quad (6)$$

Reflected quantities such as normal momentum flux and energy are found by setting  $s = 0$ , letting  $\hat{n}$  represent the local surface element, and assuming the mass flux to a surface element is conserved<sup>17</sup>.

## 2.2 Lunar Dust Generation

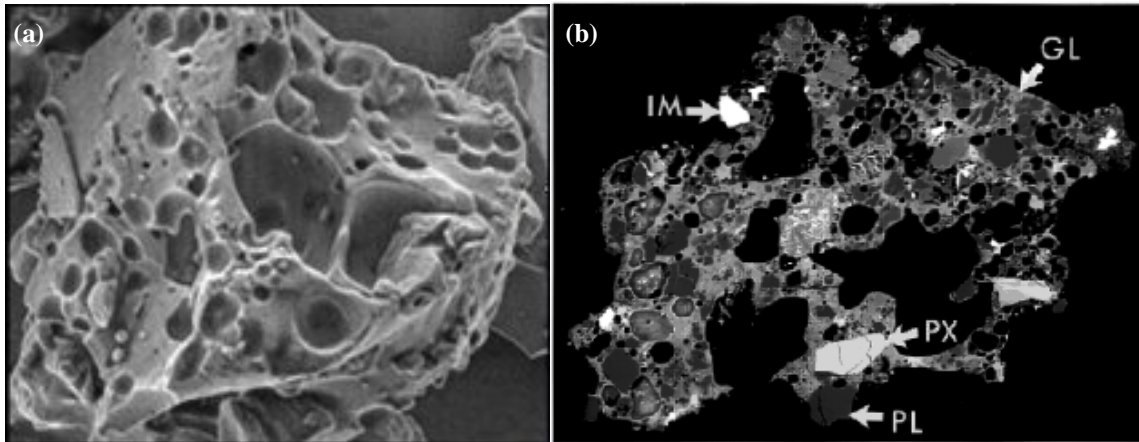


**Figure 4. Representative specimens of individual lunar dust grains; (a) whole, and (b) in cross-section<sup>18</sup> (frame width  $\approx 0.66$  mm)**

### 2.2.1 Lunar Dust Properties

Many lunar dust properties have been characterized. Lunar dust is described as a basaltic ash having a specific density of  $2.9 \text{ g/cm}^3$ , an average grain radius of roughly 70 microns, and low electrical conductivity<sup>6,18</sup>. Representative specimens of individual lunar dust grains are shown whole and in polished section in Fig. 4 above<sup>18</sup>. Dust grains tend to be highly jagged, as the lunar environment is not characterized by oxidation.

### 2.2.2 Dust Production Mechanism

A model was developed by Roberts in support of the Apollo project to describe the manner in which surface shear stress translates into surface erosion<sup>1</sup>. The original effort was undertaken in order to help predict obscuration effects the astronauts might encounter.

Regarding dust generation, it was assumed entrainment of a dust particle must overcome static friction, gravitational and cohesive forces, and the effects entrained particles might have upon one another were neglected.

$$\frac{\tau_{\text{crit}}}{\sigma g D c \cos \beta} + \tan \beta = \frac{\tau_{\text{coh}}}{\sigma g D c \cos \beta} + \tan \alpha \quad (7)$$

In Eq. 7,  $\tau_{\text{crit}}$  is the level of applied shear stress due to plume impingement just needed to budge a layer of dust having projected area  $c$ , grain diameter  $D$ , density  $\sigma$ , under lunar gravity  $g$ . Cohesive stress  $\tau_{\text{coh}}$  accounts for attractive forces possibly binding finer grains together, angle  $\beta$  represents the local angle of the surface from horizontal, and  $\tan \alpha$  is the coefficient of static friction. The rate of dust generation is<sup>1</sup>

$$\frac{u_{\text{LD}}}{2} \frac{dm''}{dt} = \tau - \tau_{\text{crit}} \quad (8)$$

In Eq. 8, shear stress  $\tau$  in excess of that needed to erode the regolith is spent accelerating particles to their final velocity<sup>1</sup>. That final velocity  $u_{\text{LD}}$  is presented as a fraction of local plume velocity  $v$ . Roberts estimated this fraction by considering viscous and pressure forces acting on the newly-entrained particle<sup>1</sup>.

A recent reference noted some erosion rates predicted using Roberts' theory lie within an order of magnitude of measured values for small-scale terrestrial experiments, but the general level of fidelity is not clear<sup>19</sup>. Verification of particle velocities were not commented upon, but it is clear that although aerodynamic effects on the freed particles dominates their trajectories, Roberts had neglected them<sup>1,13</sup>.

At any rate, a number of modifications to Roberts' model are currently being actively investigated by Metzger, *et al.*<sup>13,19,20</sup>. They identify the mechanism described above as "viscous erosion", to which they have added three other dust-generating mechanisms: "bearing capacity failure", where pressure upon the soil causes it to be pushed downwards in a narrow cup; "diffused gas eruption", where plume gas penetrates the soil and subsequently erupts, carrying dust with it; and "diffusion-driven shearing", where dust is not created as individual grains but rather due to aggregate spallation<sup>20</sup>.

## 2.3 Electrostatic Attraction

Lack of lunar atmospheric moisture exacerbates the electrical charging environment. On the sunlit side, photoelectron emission dominates the charging process, resulting in small positive potentials. In shadow, plasma currents dominate, leading to negative potentials of roughly 50-100 V<sup>21</sup>. In addition, the author also wonders

whether the action of a rocket engine plume producing dust through the mechanisms discussed above generates charging via triboelectric effects<sup>22</sup>.

The approach for assessing the amount of disturbed, charged dust that may become attracted to Altair will follow a technique developed for the NASA Space Environments & Effects (SEE) program by Gordon & Rantanen to estimate volatile species contamination associated with a particular physical mechanism<sup>23</sup>. This mechanism, referred to as Electrostatic Return Flux (ESR), occurs when such species outgassed from a spacecraft become photoionized or charged by ambient electrons and influenced by the oppositely-charged spacecraft<sup>23</sup>.

The Debye length  $\lambda$  is a characteristic value over which the plasma between the ion and a presumably charged Altair shields the strength of the electric field of the latter. One assumes that dust trajectories are initially directed radially away from the lander. It turns out that the work needed to reattract charged dust must exceed a grain's kinetic energy, leading to a critical balance:

$$\frac{m(u_{L/D})^2}{2} = \frac{qQ}{4\pi\epsilon_0} \left\{ \int_{r_{\text{crit}}}^{\infty} \frac{dr}{r^2 \exp\left[\frac{r-r_A}{\lambda}\right]} \right\}. \quad (9)$$

In this simple model, Altair is represented by a sphere based on a representative geometric dimension having radius  $r_A$ ,  $q$  and  $Q$  are the ion and spacecraft charge levels, and  $\epsilon_0$  is the permittivity of free space. Eq. (9) is to be solved for  $r_{\text{crit}}$  to find the locus of particles of a certain size and charge that become attracted to Altair.

### 3.0 Procedure

#### 3.1 Transient Plume Model

Let the reader imagine the following description refers to handling of input data  $i$  on each surface element  $j$  of a starting surface associated with a single timestep  $n$  from a given set of entrance conditions for density, velocity, and temperature. Generally at timestep  $n$ , the FM plume code reads in the elapsed time  $t_i^n$ , density  $\rho_i^n$ , velocity  $U_i^n$ , and temperature  $T_i^n$ , and assigns this information to each node  $j$  constituting the starting surface. Because individual starting surface elements may have different areas from one another, the elemental source mass increment  $\Delta m$  to be used in the FM equations is approximated by  $\Delta m_{i,j}^n$ :

$$\Delta m_{i,j}^n = \rho_i^n U_i^n \Delta A_j \frac{t_i^{n+1} - t_i^{n-1}}{2}. \quad (10)$$

At this point we have set up a transient problem to determine how the state of the input source gas  $i$  at timestep  $n$  will influence solution elements  $k$  at times greater than  $t_i^n$ . Using another time counter  $m$  for solution time  $t^m \equiv t - t_i^n$ , it is  $t^m$  that is employed in Eqns. 4 & 5 to compute  $p_{\perp,k}^m$  and  $\tau_k^m$ . The transient solution is run out to some arbitrary final time (Fig. 5 below).

Effective surface stresses acting at points  $k$  due to plume impingement at a given elapsed time  $t^m$  become the superposition in time of the influences from nozzle exit elements for all previous timesteps.

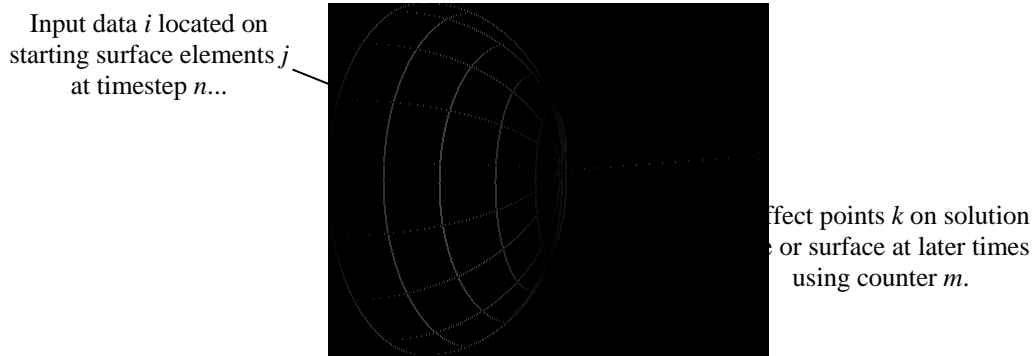


**Figure 5. Schematic representation of starting surface and radial solution line**

### 3.2 Dust Generation Rate

As a transient flowfield associated with descent engine shut-off is built up, one may use this solution to estimate time-dependent rates of dust production using the mechanism described in Section 2.2.2. (It should be noted that as current research into dust generation mechanisms becomes translated into mathematical models, one should expect this description to change accordingly.)

For the individual dust particle generation rate described in Section 2.2.2, it seems possible to work with a given distribution of particle sizes instead of an average value, determining the mass generation rate and velocity  $u_{L/D}$  for each “bin” of given particle size and size width separately, and feeding this information into the electrostatic attraction model.

### 3.3 Electrostatic Attraction

Using the transient plume solution, and binning particle sizes to approximate their effects on Altair particulate contamination, one may estimate the cumulative level of deposition on critical surfaces. The model for electrostatic attraction is also size-dependent, through the kinetic energy associated with a lofted particle used to determine  $r_{crit}$ .

As a flux of attracted particles reaches Altair surfaces, a percent area coverage (PAC) may be calculated. Conservative PAC values for a given level of dust attraction would tend to overestimate the influence of individual particles and underestimate the underlying base area associated with the critical surface. Worst-case PAC assumes no overlap of particulate matter, so each particle’s complete projected area may count towards obscuration. Flat radiator surfaces are representative of near-worst case circumstances, since they are more adequately defined by projected faces of the vehicle. Assuming Altair’s actual surface area is described by simple projections conservatively neglects contributions such as shadowed regions and surfaces having local rather than global curvature, among other things.

### 4.0 Concluding Remarks

Constellation mission managers are rightly concerned about the effects of dust-related contamination for the Altair Lunar Lander. The purpose of this paper was to describe a concept for modeling the lunar dust-generated environment associated with lunar descent engine operations during the first Altair landing.



Certain curious properties of lunar dust in the high-vacuum lunar environment were described, including charging. A quick review of designated descent engine parameters indicates lunar dust stirred up by the exhaust plume will be accelerated away from Altair so vigorously that the effects of attraction should be negligible—while the engine is running. During the shutdown transient, plume product momentum will decay rapidly, while still creating enough surface stress to loosen some dust from the lunar regolith. It is during this period that such particles may become attracted to the Lunar Lander.

The manner in which charged particles may attract themselves to the Lander was discussed, along with a conservative description of how this contaminant might be evaluated in terms of Percent Area Coverage.

The author recognizes that current studies of dust properties, plume impingement of the lunar surface, and plume-induced soil erosion may produce enhanced models that should be taken into account, so the discussion presented here should be seen as a first cut approximation of a difficult problem.

## 5.0 Acknowledgements

The author gratefully acknowledges support from NASA Contract NNG07CA21C and SGT, Inc.

## 6.0 References

<sup>1</sup>Roberts, L., “The interaction of a rocket exhaust with the lunar surface”, *The Fluid Dynamic Aspects of Space Flight, AGARDograph 87*, Vol. II, Gordon & Breach, 269-290, 1996.

<sup>2</sup>Stark, R., *et al.*, “Lunar Dust/Debris Hazards Associated with the Manned Flying System”, *NASA CR-61106*, NASA-Marshall Space Flight Center, N66-10703, October 1965.

<sup>3</sup>Gaier, J., “The Effects of Lunar Dust on EVA Systems During the Apollo Missions”, *NASA TM-2005-213610*, NASA-Glenn Research Center, March 2005.

<sup>4</sup>Gaier, J., and Jaworske, D., “Lunar Dust on Heat Rejection System Surfaces: Problems and Prospects”, *NASA/TM-2007-214814*, NASA-Glenn Research Center, 6 June 2007.

<sup>5</sup>Wagner, S., “The Apollo Experience Lessons Learned for Constellation Lunar Dust Management”, *NASA/TP-2006-213726*, NASA-Johnson Space Center, October 2006.

<sup>6</sup>Stubbs, T., *et al.*, “Impact of Lunar Dust on the Exploration Initiative”, presented at the 36<sup>th</sup> *Lunar and Planetary Science Conference*, League City, TX, 14-18 March 2005.

<sup>7</sup>*NASA Constellation Main Home Page*, <[http://www.nasa.gov/mission\\_pages/constellation/main/](http://www.nasa.gov/mission_pages/constellation/main/)>, B. Dunbar responsible contact, 9 May 2008, last retrieved 2 June 2008.

<sup>8</sup>“NASA’s Exploration Systems Architecture Study”, Final Report, *NASA-TM-2005-214062*, November 2005.

<sup>9</sup>Morring, F., Jr., “Heavier Still—NASA needs bigger Ares V to meet lunar requirements”, *Aviation Week & Space Technology*, 34-35, 3 March 2008.

<sup>10</sup>Winter, F., & van der Linden, R., “Out of the Past”, *Aerospace America*, 44-45, April 2007.

<sup>11</sup>“RL-10A-4”, *Encyclopedia Astronautica*, <<http://www.astronautix.com/engines/rl10a4.htm>>, M. Wade responsible contact, last retrieved 10 March 2008.

<sup>12</sup>“Apollo Lunar Landing”, *Encyclopedia Astronautica*, < <http://www.astronautix.com/craft/aponding.htm>>, M. Wade responsible contact, last retrieved 3 June 2008.

<sup>13</sup>Immer, C., *et al.*, “Apollo Video Photogrammetry Estimation Of Plume Impingement Effects”, presented at the *11<sup>th</sup> ASCE Aerospace Division International Conference on Engineering, Science, Construction, and Operation in Challenging Environments*, Long Beach, CA, 3-5 March 2008.

<sup>14</sup>Lumpkin, F., *et al.*, “Plume Impingement to the Lunar Surface: A Challenging Problem for DSMC”, presented at the *Direct Simulation Monte Carlo, Theory, Methods, and Applications Conference*, Santa Fe, NM, 30 September – 3 October 2007.

<sup>15</sup>Woronowicz, M., *Proceedings of the 22<sup>nd</sup> Intl. Symposium on Rarefied Gas Dynamics*, American Institute of Physics, AIP Conf. Proceedings Vol. 585, Melville, NY, 798-805, 2001.

<sup>16</sup>Woronowicz, M., *Proceedings of the 23<sup>rd</sup> Intl. Symposium on Rarefied Gas Dynamics*, American Institute of Physics, AIP Conf. Proceedings Vol. 663, Melville, NY, 588-594, 2003.

<sup>17</sup>Woronowicz, M., *Proceedings of the 24<sup>th</sup> Intl. Symposium on Rarefied Gas Dynamics*, American Institute of Physics, AIP Conf. Proceedings Vol. 762, Melville, NY, 431-436, 2005.

<sup>18</sup>McKay, D., *et al.*, “JSC-1: A New Lunar Soil Simulant”, *Engineering, Construction, and Operations in Space IV*, American Society of Civil Engineers, pp. 857-866, 1994.

<sup>19</sup>Metzger, P., *et al.*, “Modification of Roberts’ Theory for Rocket Exhaust Plumes Eroding Lunar Soil”, presented at the *11<sup>th</sup> ASCE Aerospace Division International Conference on Engineering, Science, Construction, and Operation in Challenging Environments*, Long Beach, CA, 3-5 March 2008.

<sup>20</sup>Metzger, P., *et al.*, “Cratering and Blowing Soil by Rocket Engines During Lunar Landings,” to be presented at the *6<sup>th</sup> International Conference on Case Histories in Geotechnical Engineering*, Arlington, VA, 11-16 August 2008.

<sup>21</sup>Halekas, J., *et al.*, “Lunar Electric Fields and Dust: Implications for In Situ Resource Utilization”, presented at the *36<sup>th</sup> Lunar and Planetary Science Conference*, League City, TX, 14-18 March 2005.

<sup>22</sup>Dettleff, G., personal communication, 17-18 November 2003.

<sup>23</sup>Gordon, T., Rantanen, R., “Electrostatic Return of Contaminants”, NASA Marshall Space Flight Center Contracts PO H-32496D and PO H-32497D Final Report, 5 March 2003.